iScience

CellPress
OPEN ACCESS

Article

CircZNF609/miR-324-5p/voltage-dependent anion channel 1 axis promotes malignant progression of ovarian cancer cells

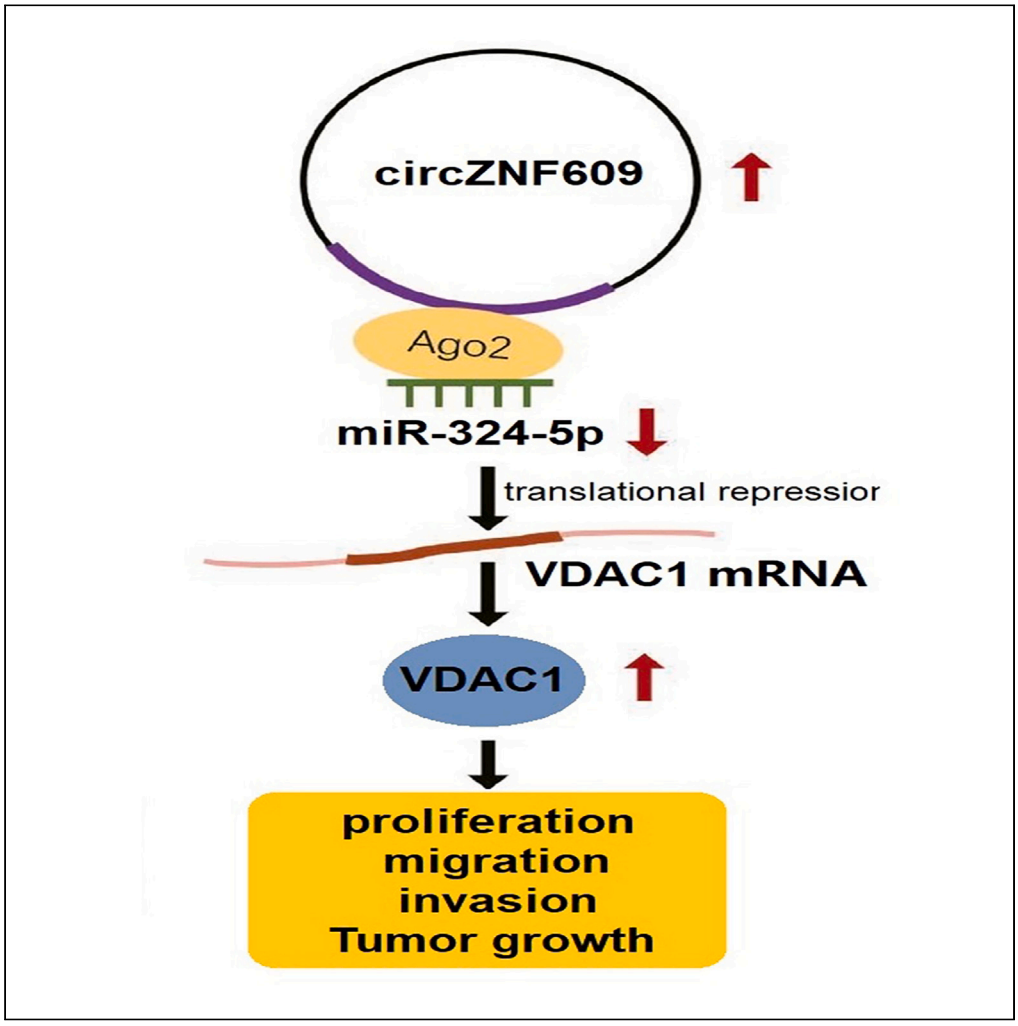

Lina Ren, Xiaoxi Huo, Yi Zhao

zhaoyicmu@sina.com

Highlights

CircZNF609 is upregulated in OC and related to metastasis and prognosis

CircZNF609 triggers proliferation, migration and invasion of OC cells

CircZNF609 promotes malignant phenotypes of OC cells via miR-324-5p/VDAC1

Ren et al., iScience 27, 110861
November 15, 2024
Published by Elsevier Inc.
https://doi.org/10.1016/j.isci.2024.110861

iScience

CellPress
OPEN ACCESS

Article

CircZNF609/miR-324-5p/voltage-dependent anion channel 1 axis promotes malignant progression of ovarian cancer cells

Lina Ren,[1] Xiaoxi Huo,[2] and Yi Zhao[1,3,*]

SUMMARY

The dysregulation of circular RNAs (circRNAs) has been associated with OC development and progression. This study investigated the role of circZNF609 in ovarian cancer (OC) by analyzing its impact on cell proliferation, migration, and invasion. Initially, the study assessed the expression of circZNF609 in OC tissues and adjacent normal tissues. The results revealed elevated circZNF609 levels in OC tissues and cell lines, correlating with poor prognosis, lymph node metastasis, and advanced clinical stage. Subsequently, *in vitro* and *in vivo* experiments were conducted to elucidate the biological functions of circZNF609 in OC progression. The findings showed that the knockdown of circZNF609 resulted in reduced OC cell proliferation, migration, invasion, and tumor growth. Mechanistically, circZNF609 was identified to function as a sponge for miR-324-5p, thereby upregulating voltage-dependent anion channel 1 (VDAC1) expression and promoting OC progression. Our findings indicate that circZNF609 promotes OC via the miR-324-5p/VDAC1 axis, contributing to the therapeutic targeting of this disease.

INTRODUCTION

Ovarian cancer (OC), the deadliest among gynecological cancers, constituted 3.7% of female cancer diagnoses and 4.7% of cancer-related deaths in 2020, with a five-year survival rate of approximately 30%.[1] The current treatment paradigm for OC involves surgical interventions, such as radical resection or cytoreductive surgery, followed by chemotherapy.[2] However, the emergence of chemotherapeutic resistance is a leading cause of treatment failure and disease recurrence.[3,4] Therefore, there is a pressing need for innovative diagnostic methods and treatments that facilitate the early detection of OC. In recent years, a more profound understanding of the molecular mechanisms driving OC, along with advancements in its treatment, has opened the door to the development of targeted therapeutics. This evolution is crucial for improving prognostic outcomes in patients with OC.

Circular RNAs (circRNAs) represent a class of non-coding RNAs that originate from precursor mRNA transcripts and are characterized by their covalently closed, single-stranded circular structure.[5] Initially discovered in eukaryotic organisms in the 1970s,[6] the functional roles and applications of circRNAs in various diseases have been increasingly elucidated with the advent of high-throughput sequencing and bioinformatics technologies in recent years.[7,8] Research has demonstrated that circRNAs can modulate gene expression through various mechanisms, including acting as sponges for miRNAs, interacting with mRNA molecules, directly binding to proteins, and encoding short peptides, thereby influencing disease progression.[9,10] Accumulating evidence indicates that circRNAs may influence the biological behaviors of tumor cells, including proliferation, invasion, and apoptosis, suggesting their potential as therapeutic targets and prognostic markers.[11,12] In the context of OC, circRNAs can function as miRNA sponges to regulate gene expression.[13,14] In this study, we explored the role and significance of circZNF609 in OC. CircZNF609 (hsa_circ_0000615) is located at the position of chr15:64791491–64792365 and has a genomic length of 874 nucleotides.

Its dysregulation has been associated with various malignancies, including hepatocellular carcinoma,[15] cervical cancer,[16] breast cancer,[17] prostate cancer,[18,19] gastric cancer,[20,21] lung cancer[22,23] and glioma.[24,25] However, its specific role in the pathogenesis of OC has not been fully established.

Previous research has underscored the pivotal roles of dysregulated miRNA expression in the initiation and progression of cancer.[26] MiRNAs exert their regulatory functions by complementarily base pairing with the 3′ untranslated region (3′ UTR) of mRNAs, resulting in either mRNA degradation or inhibition of protein translation.[27] Moreover, the tumor-suppressive effects of miR-324-5p have been substantiated in several types of malignancies, including glioma,[28,29] gastric cancer,[30,31] and OC.[32,33] Given these findings, a comprehensive exploration of the role of miR-324-5p in OC is essential.

[1]Department of Obstetrics, The First Hospital of China Medical University, Liaoning 110001, China
[2]Department of Obstetrics and Gynecology, The Seventh Medical Center of PLA General Hospital, Beijing 100700, China
[3]Lead contact
*Correspondence: zhaoyicmu@sina.com
https://doi.org/10.1016/j.isci.2024.110861

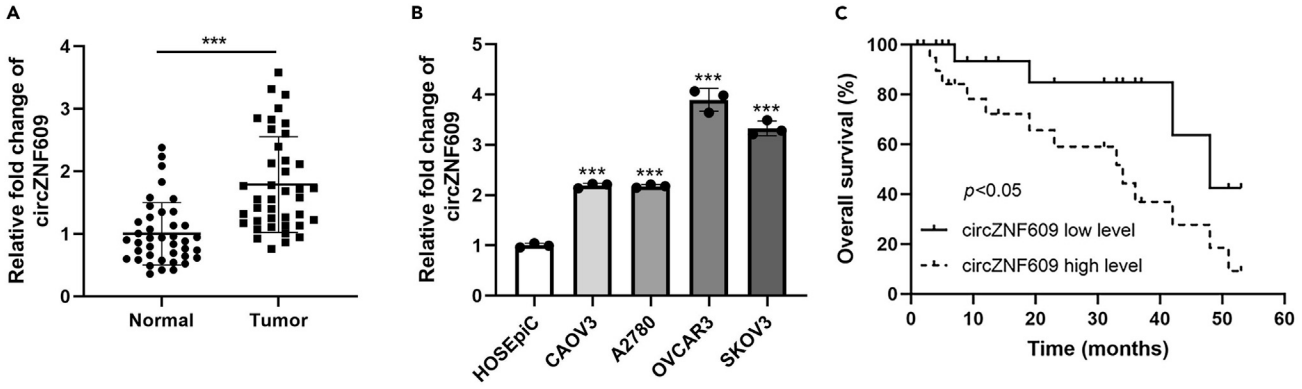

Figure 1. CircZNF609 is upregulated in OC tissues and cells

(A) CircZNF609 expression in 40 pairs of OC and adjacent normal tissues was determined using qRT-PCR.

(B) CircZNF609 expression in four OC (CAOV3, A2780, OVCAR3 and SKOV3) cell lines and normal ovarian epithelial HOSEpic cell line was measured using qRT-PCR.

(C) High expression levels of circZNF609 were associated with shorter overall survival of patients with OC. All data were presented as the mean ± SD of three independent experiments. ***$p < 0.001$ vs. Normal or HOSEpic.

Voltage-dependent anion channel 1 (VDAC1) is a key regulator of mitochondrial function, and its targeting offers significant therapeutic potential for modulating the biology of cancer and other diseases.[34] A recent study has shown that peroxisome proliferator-activated receptor gamma coactivator 1-alpha (PGC1α) can reduce apoptosis by activating the HSP70/HK2/VDAC1 signaling pathway, thereby contributing to cisplatin resistance in OC.[35] Therefore, further research into the molecular mechanisms of VDAC1 in OC is crucial. Bioinformatics prediction websites suggest that miR-324-5p may share the same binding sites with circZNF609 and VDAC1. Therefore, we hypothesized that circZNF609 may act as competing endogenous RNA (ceRNA) to regulate the miR-324-5p/VDAC1 axis, thereby participating in the regulation of OC progression.

In this study, we observed that circZNF609 is overexpressed in OC, indicating its potential as a key regulator in OC development. By leveraging bioinformatics tools, we demonstrated that circZNF609 modulates VDAC1 expression in OC through interaction with miR-324-5p. This led us to hypothesize that the circZNF609/miR-324-5p/VDAC1 axis is crucial in the cellular progression of OC. Our findings elucidate the molecular mechanisms of OC pathogenesis and offer potential therapeutic targets for OC treatment.

RESULTS

CircZNF609 is upregulated in ovarian cancer tissues and cells

To elucidate the expression profile of circZNF609 in OC tissues and cell lines, quantitative real-time PCR (qRT-PCR) was employed to quantify circZNF609 levels in a cohort of 40 OC specimens and their normal counterparts. Our findings revealed a marked upregulation of circZNF609 in OC tissues relative to normal tissues (Figure 1A; $p < 0.001$), suggesting a potential oncogenic role for this circRNA in OC pathogenesis. Moreover, the expression of circZNF609 was assessed in four OC cell lines (CAOV3, A2780, OVCAR3, and SKOV3) and compared to that in HOSEpic cells. The results indicated a significantly elevated expression of circZNF609 in all OC cell lines tested (Figure 1B; $p < 0.001$), further supporting the hypothesis that circZNF609 may contribute to OC progression. The prognostic significance of circZNF609 was also investigated. Kaplan-Meier survival analysis demonstrated that higher circZNF609 expression was associated with reduced survival rates in patients with OC (Figure 1C), underscoring the potential utility of circZNF609 as a prognostic biomarker. To explore the clinical relevance of circZNF609 expression, tumor samples were stratified into low and high expression groups based on circZNF609 levels. Correlation analysis with clinicopathological features revealed that elevated circZNF609 expression was significantly correlated with lymph node metastasis and advanced International Federation of Gynecology and Obstetrics (FIGO) stage (Table S1; $p < 0.05$). These findings collectively suggest that circZNF609 is not only associated with OC development but also plays a significant role in the progression of this malignancy.

Silencing of circZNF609 inhibits aggressive behaviors in ovarian cancer cells and tumor growth *in vivo*

To elucidate the functional significance of circZNF609 in the progression of OC, we employed a targeted shRNA-mediated knockdown approach in OVCAR3 and SKOV3 cell lines, which exhibit high endogenous circZNF609 expression. The efficacy of circZNF609 silencing was confirmed by qRT-PCR, with sh-circZNF609#1 demonstrating the most pronounced reduction in circZNF609 levels (Figure 2A; $p < 0.001$). Functional assays were subsequently conducted to assess the impact of circZNF609 knockdown on OC cell proliferation. Cell counting kit-8 (CCK-8) and 5-ethynyl-2′-deoxyuridine (EdU) incorporation assays revealed a significant decrease in cell viability and EdU-positive cells in both OVCAR3 and SKOV3 cell lines following circZNF609 knockdown (Figures 2B and 2C; $p < 0.001$ and $p < 0.01$, $p < 0.001$, respectively), indicating an anti-proliferative effect of circZNF609 suppression. Moreover, Transwell migration and invasion assays demonstrated that circZNF609 downregulation led to a marked reduction in the migratory and invasive capabilities of OC cells (Figures 2D and

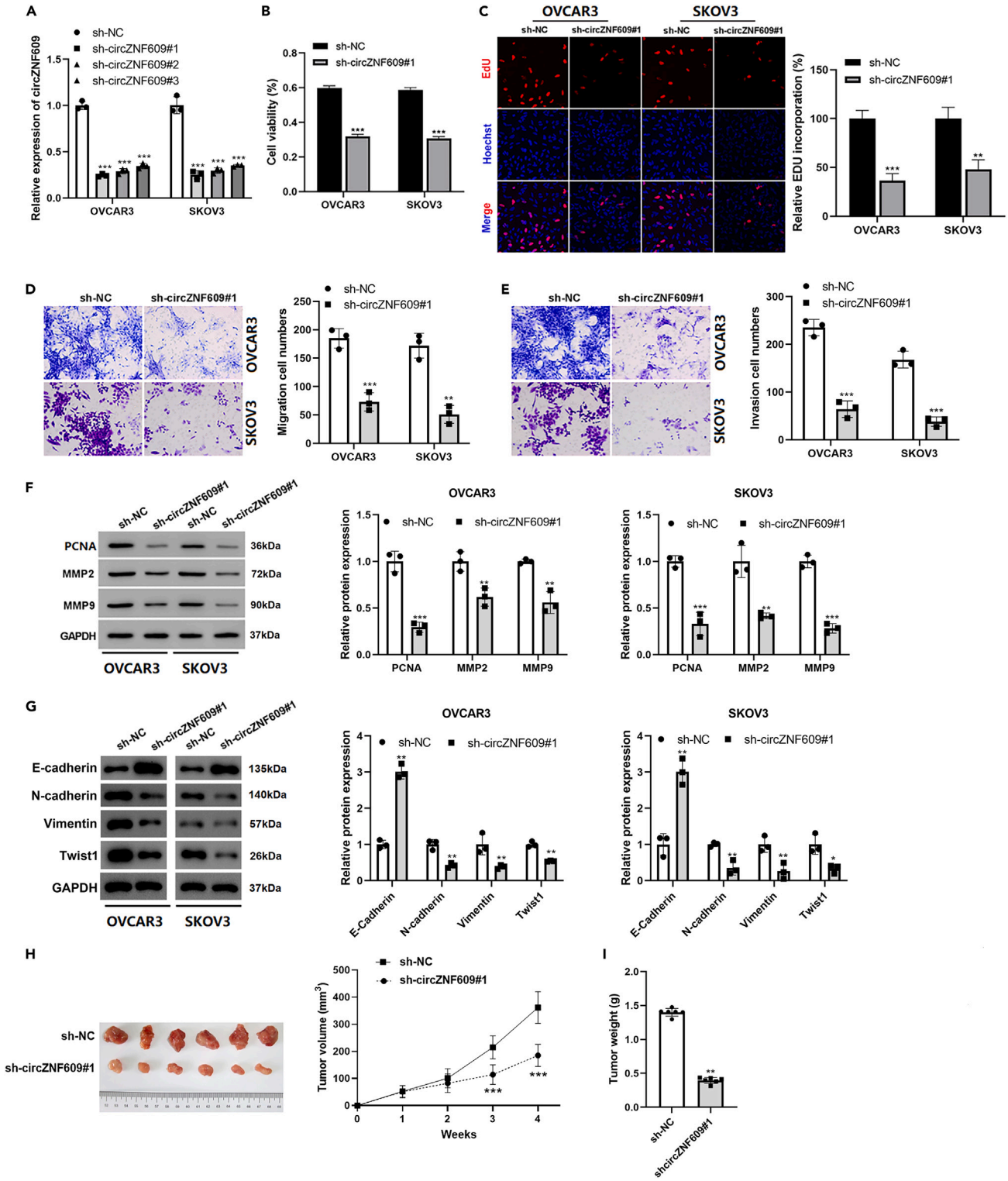

Figure 2. Silencing of circZNF609 inhibits proliferation, migration, and invasion in OC cells and tumor growth *in vivo*

(A) The transfection efficiency of circZNF609 shRNA was measured by qRT-PCR. The effects of circZNF609 knockdown on cell proliferation were measured by CCK-8 assay (B) and EdU assay (C) in OVCAR3 and SKOV3 cells. The effects of circZNF609 knockdown on cell migration (D) and invasion (E) were measured by Transwell assays in OVCAR3 and SKOV3 cells.

(F) The protein levels of PCNA, MMP-2, and MMP-9 were measured by western blotting in OVCAR3 and SKOV3 cells after circZNF609 silencing.

Figure 2. *Continued*

(G) The protein levels of E-cadherin, N-cadherin, Vimentin, and Twist1 were measured by western blotting in OVCAR3 and SKOV3 cells after circZNF609 silencing. (H and I) SKOV3 cells transfected with sh-NC or sh-circZNF609#1 were subcutaneously injected into nude mice ($N = 6$ per group), and then the representative photographs of xenograft tumors were shown; the tumor volume and weight were assessed. All data were presented as the mean ± SD of three independent experiments. *$p < 0.05$, **$p < 0.01$, ***$p < 0.001$ vs. sh-NC.

2E; $p < 0.01$, $p < 0.001$). These findings were corroborated by immunoblotting analysis, which revealed a concomitant decrease in the expression of proliferating cell nuclear antigen (PCNA), matrix metalloproteinase 2 (MMP-2), matrix metalloproteinase 9 (MMP-9), indicative of reduced proliferation, migration, and invasion (Figure 2F; $p < 0.01$, $p < 0.001$). The levels of epithelial-mesenchymal transition (EMT) markers were further evaluated by Western blot. The data showed that the downregulation of Twist1 expression induced by circZNF609 knockdown blocked EMT, characterized by a notable increase in the expression of the epithelial marker E-cadherin, coupled with a concomitant decrease in the mesenchymal markers N-cadherin and Vimentin, in both OVCAR3 and SKOV3 cell lines (Figure 2G; $p < 0.05$, $p < 0.01$, $p < 0.001$). This evaluation underscores the pivotal role of circZNF609 in regulating EMT and highlights the potential therapeutic implications of targeting this pathway in OC. To further validate the role of circZNF609 in OC tumorigenesis *in vivo*, we established a xenograft tumor model using nude mice. Upon circZNF609 silencing, a significant reduction in tumor volume and weight was observed (Figures 2H and 2I; $p < 0.01$, $p < 0.001$), underscoring the suppressive effect of circZNF609 inhibition on OC progression both *in vitro* and *in vivo*. Collectively, these results provide compelling evidence that circZNF609 plays a critical role in OC progression and suggest that targeting circZNF609 may represent a potential therapeutic strategy for the management of this malignancy.

CircZNF609 sequesters miR-324-5p in ovarian cancer cells

To elucidate the molecular mechanisms underlying the role of circZNF609 in OC, we employed bioinformatics tools to predict potential target miRNAs of circZNF609. Our analysis identified miR-324-5p as a putative target of circZNF609 (Figure 3A). To validate this interaction, we performed a luciferase reporter assay, which demonstrated that miR-324-5p mimics significantly reduced the luciferase activity of the wild-type circZNF609 reporter construct compared to the mutant construct (Figure 3B; $p < 0.01$), indicating a direct interaction between circZNF609 and miR-324-5p. Furthermore, we observed that transfection with miR-324-5p mimics led to a significant increase in miR-324-5p expression in OVCAR3 and SKOV3 cells (Figure 3C; $p < 0.001$), confirming the upregulation of miR-324-5p by miR-324-5p mimics. The binding relationship between circZNF609 and miR-324-5p was further substantiated by an RNA pull-down assay (Figure 3D; $p < 0.001$). To investigate the regulatory role of circZNF609 on miR-324-5p expression, we silenced circZNF609 in OVCAR3 and SKOV3 cells. Our results showed that circZNF609 knockdown resulted in a significant increase in miR-324-5p expression (Figure 3E; $p < 0.001$), suggesting that circZNF609 negatively regulates miR-324-5p expression. Additionally, we found that miR-324-5p was downregulated in OC tissues compared to normal tissues (Figure 3F; $p < 0.001$), and its expression was inversely correlated with circZNF609 levels (Figure 3G; $p < 0.05$, $r^2 = 0.7222$). These findings collectively indicate that circZNF609 functions as a ceRNA by sponging miR-324-5p in OC, thereby modulating its expression.

Overexpression of miR-324-5p inhibits ovarian cancer progression *in vitro*

To further elucidate the biological impact of miR-324-5p on OC progression, we conducted a series of functional assays following the transfection of miR-324-5p mimics or a negative control (miR-NC) into OVCAR3 and SKOV3 cell lines. Our findings indicated that the enforced expression of miR-324-5p resulted in a substantial reduction in cell viability (as depicted in Figure 4A; $p < 0.01$), a decrease in the number of Edu-positive proliferating cells (Figure 4B; $p < 0.05$, $p < 0.01$), and a marked inhibition of cellular migration (Figure 4C; $p < 0.01$) and invasion (Figure 4D; $p < 0.01$). These results underscore the tumor-suppressive function of miR-324-5p in the context of OC, suggesting its potential as a therapeutic target for OC.

MiR-324-5p targets voltage-dependent anion channel 1 in ovarian cancer cells

To elucidate the downstream regulatory mechanisms of miR-324-5p in OC, we utilized the Encyclopedia of RNA interactomes (ENCORI) prediction tool to identify potential target genes. Among the predicted targets, we focused on VDAC1, an oncogene previously implicated in cancer progression, including OC (Figure 5A). To validate the interaction between miR-324-5p and VDAC1, we conducted a luciferase reporter assay. The results showed that miR-324-5p mimics significantly reduced the luciferase activity of the VDAC1 wild-type reporter construct (Figure 5B; $p < 0.001$), confirming the direct binding of miR-324-5p to VDAC1. Subsequent real-time PCR and Western blot analyses demonstrated that the overexpression of miR-324-5p significantly downregulated VDAC1 expression at both the mRNA and protein levels (Figures 5C and 5D; $p < 0.01$, $p < 0.001$). In OC tissues, VDAC1 mRNA expression was found to be elevated (Figure 5E; $p < 0.001$) and negatively correlated with miR-324-5p expression (Figure 5F; $p < 0.05$, $r^2 = 0.5670$). Furthermore, VDAC1 expression was inversely correlated with miR-324-5p (Figure 5F; $p < 0.05$, $r^2 = 0.5670$) and positively correlated with circZNF609 expression in OC tissues (Figure 5G; $p < 0.05$, $r^2 = 0.7090$). To further investigate the regulatory role of miR-324-5p on VDAC1, we transfected OVCAR3 and SKOV3 cells with anti-miR-324-5p to inhibit endogenous miR-324-5p expression. This transfection significantly reduced miR-324-5p expression (Figure 5H; $p < 0.001$). Moreover, the silencing of circZNF609 downregulated VDAC1 protein levels, and this effect was reversed by the addition of anti-miR-324-5p in OVCAR3 and SKOV3 cells (Figure 5I; $p < 0.01$, $p < 0.001$). Collectively, these findings indicate that miR-324-5p directly targets VDAC1 in OC cells, suggesting a regulatory axis involving circZNF609, miR-324-5p, and VDAC1 that may play a critical role in OC progression.

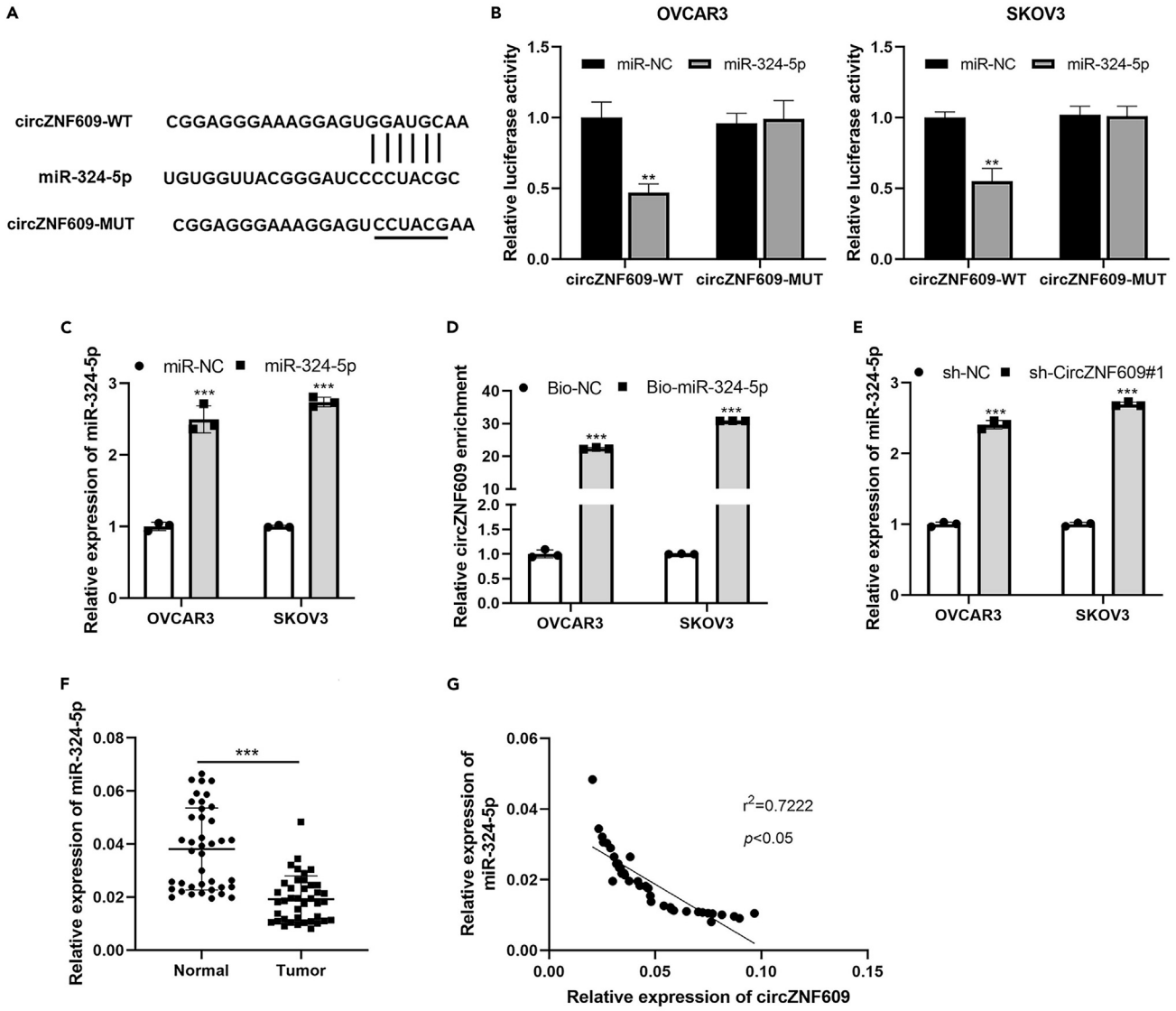

Figure 3. CircZNF609 sequesters miR-324-5p in OC cells

(A) The predicted binding sites of miR-324-5p to circZNF609 sequences were predicted by CircInteractome.

(B) Luciferase activities were detected in OVCAR3 and SKOV3 cells co-transfected miR-324-5p mimics or miR-NC with circZNF609-WT or -MUT. $^{**}p < 0.01$ vs. miR-NC.

(C) The transfection efficiency of miR-324-5p overexpression was measured by qRT-PCR. $^{***}p < 0.001$ vs. miR-NC.

(D) RNA pull down assay was used to determine the binding relationship between circZNF609 and miR-324-5p. $^{***}p < 0.001$ vs. Bio-NC.

(E) miR-324-5p expression was measured by qRT-PCR in OVCAR3 and SKOV3 cells after circZNF609 silencing. $^{***}p < 0.001$ vs. sh-NC.

(F) miR-324-5p expression in 40 pairs of OC and adjacent normal tissues was determined using qRT-PCR. $^{***}p < 0.001$ vs. Normal.

(G) The expression correlation of miR-324-5p with circZNF609 in OC tissues was analyzed by Pearson's correlation analysis. $p < 0.05$. All data were presented as the mean ± SD of three independent experiments.

CircZNF609 promotes the malignant evolution of ovarian cancer cells via miR-324-5p/voltage-dependent anion channel 1 axis

To further delineate the functional significance of the circZNF609-miR-324-5p-VDAC1 regulatory network in OC development, we conducted rescue experiments by restoring VDAC1 expression or downregulating miR-324-5p in circZNF609-silenced OVCAR3 and SKOV3 cells. The transfection of a VDAC1 overexpression plasmid resulted in a significant increase in VDAC1 protein levels (Figure 6A; $p < 0.001$), confirming the successful restoration of VDAC1 expression. Subsequent functional assays revealed that the inhibition of miR-324-5p or the upregulation of VDAC1 could abrogate the suppressive effects of circZNF609 knockdown on cell proliferation, migration, and invasion. The number of surviving cells was significantly increased (Figure 6B; $p < 0.001$), as were the numbers of EdU-positive cells (Figure 6C; $p < 0.01$, $p < 0.001$),

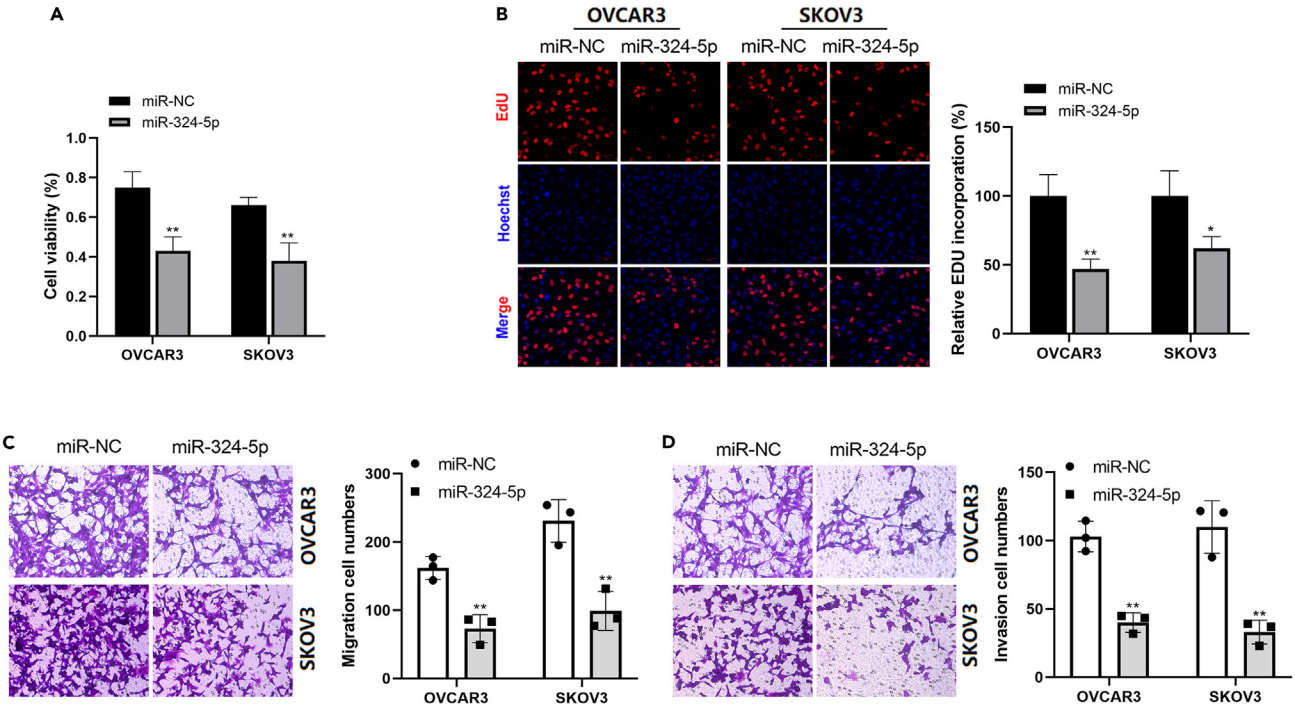

Figure 4. Overexpression of miR-324-5p inhibits OC progression *in vitro*

(A–D) The effects of miR-324-5p overexpression on cell proliferation were measured by CCK-8 assay (A) and EdU assay (B) in OVCAR3 and SKOV3 cells. The effects of miR-324-5p overexpression on cell migration (C) and invasion (D) were measured by Transwell assays in OVCAR3 and SKOV3 cells. All data were presented as the mean ± SD of three independent experiments. *$p < 0.05$, **$p < 0.01$ vs. miR-NC.

indicating a restoration of proliferative capacity. Similarly, the migratory (Figure 6D; $p < 0.01$, $p < 0.001$) and invasive (Figure 6E; $p < 0.05$, $p < 0.001$) capabilities of the cells were also enhanced, suggesting a reversal of the inhibitory effects on cell motility. Immunoblotting analysis confirmed that the downregulation of PCNA, MMP-2, and MMP-9, which were observed following circZNF609 knockdown, could be rescued by either miR-324-5p knockdown or VDAC1 overexpression (Figure 6F; $p < 0.05$, $p < 0.01$, $p < 0.001$). Taken together, these findings provide compelling evidence that circZNF609 can regulate VDAC1 expression through sponging miR-324-5p in OC, thereby influencing key cellular processes such as proliferation, migration, and invasion. These results underscore the importance of the circZNF609-miR-324-5p-VDAC1 axis in the progression of OC and suggest potential therapeutic targets for this devastating disease.

CircZNF609/miR-324-5p/voltage-dependent anion channel 1 axis regulated ovarian cancer progression *in vivo*

To elucidate the intricate regulatory interplay of the circZNF609/miR-324-5p/VDAC1 axis in OC progression, we conducted an *in vivo* rescue experiment in nude mice. Our findings from the SKOV3 cell xenograft model revealed that the downregulation of circZNF609 led to a significant reduction in tumor volume and weight. This effect was notably reversed upon the knockdown of miR-324-5p or the overexpression of VDAC1, as evidenced by the data presented in Figures 7A and 7B ($p < 0.05$, $p < 0.01$, $p < 0.001$). Moreover, the knockdown of circZNF609 was associated with an upregulation of miR-324-5p and a downregulation of VDAC1. Conversely, the suppression of miR-324-5p or the overexpression of VDAC1 counteracted these changes, as illustrated in Figures 7C and 7D ($p < 0.01$, $p < 0.001$). Collectively, the results from our nude mouse tumor model underscore the pivotal role of circZNF609 in modulating the miR-324-5p/VDAC1 axis, thereby attenuating OC progression *in vivo*. This study provides compelling evidence for the therapeutic potential of targeting the circZNF609/miR-324-5p/VDAC1 axis in the management of OC.

DISCUSSION

The current study has identified circZNF609 as a pivotal molecular biomarker that modulates the aggressive behaviors of OC cells. We have uncovered a potential regulatory mechanism, the circZNF609/miR-324-5p/VDAC1 axis, which plays a significant role in OC development. This research not only enhances our comprehension of the pathogenesis of OC but also presents promising diagnostic and therapeutic targets for this disease.

OC is the third most prevalent gynecological malignancy, leading to substantial mortality rates among women.[36,37] A growing body of evidence suggests that numerous circRNAs are emerging as significant players in the malignant biology of tumors, with the dysregulation of tumor-specific circRNAs potentially indicating the progression of various malignancies, including OC.[38] CircZNF609 has been extensively

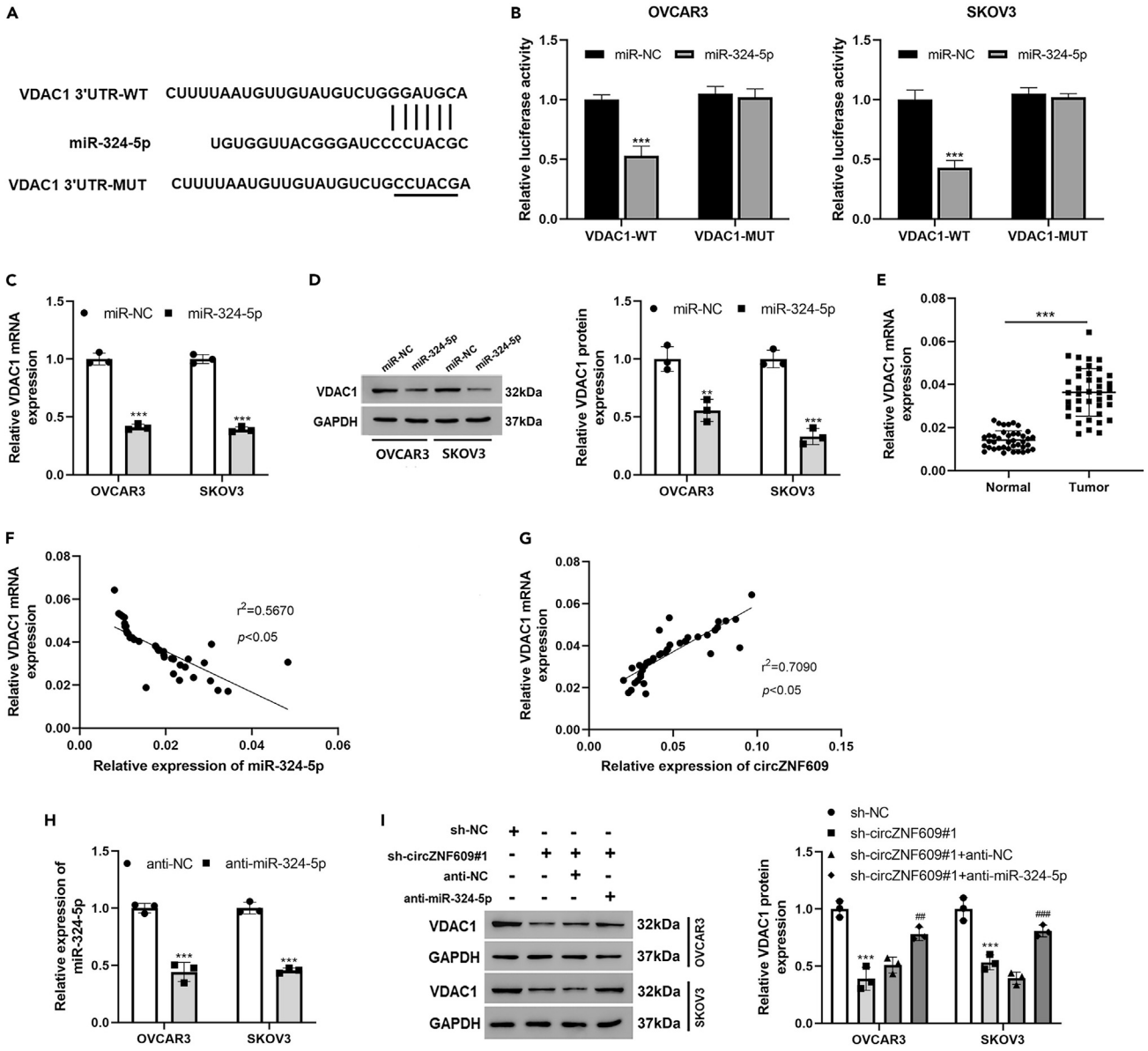

Figure 5. MiR-324-5p targets VDAC1 in OC cells

(A) The predicted binding sites of miR-324-5p to VDAC1 3'-UTR sequences were predicted by starBase.

(B) Luciferase activities were detected in OVCAR3 and SKOV3 cells co-transfected miR-324-5p mimics or miR-NC with VDAC1 3'-UTR-WT or -MUT. ***$p < 0.001$ vs. miR-NC.

(C and D) VDAC1 mRNA and protein levels were measured by qRT-PCR and western blotting in OVCAR3 and SKOV3 cells after miR-324-5p overexpression. **$p < 0.01$; ***$p < 0.001$ vs. miR-NC.

(E) VDAC1 mRNA expression in 40 pairs of OC and adjacent normal tissues was determined using qRT-PCR. ***$p < 0.001$ vs. Normal.

(F) The expression correlation of miR-324-5p with VDAC1 mRNA level in OC tissues was analyzed by Pearson's correlation analysis.

(G) The expression correlation of circZNF609 expression with VDAC1 mRNA level in OC tissues was analyzed by Pearson's correlation analysis.

(H) The transfection efficiency of miR-324-5p silencing was measured by qRT-PCR. ***$p < 0.001$ vs. anti-NC.

(I) VDAC1 protein levels were measured by western blotting in OVCAR3 and SKOV3 cells after circZNF609 or/and miR-324-5p knockdown. All data were presented as the mean ± SD of three independent experiments. ***$p < 0.001$ vs. sh-NC; $^{\#\#}p < 0.01$, $^{\#\#\#}p < 0.001$ vs. sh-circZNF609#1+anti-NC.

documented in various reproductive malignancies, where it has been implicated in promoting tumor growth, metastasis, radioresistance, and inhibiting apoptosis.[16–19] Our research team has found that circZNF609 was overexpressed in OC tissues and cell lines. Elevated levels of circZNF609 correlated with poor prognosis, suggesting its potential as a diagnostic marker for the early detection of OC and as a therapeutic target. Moreover, the suppression of circZNF609 expression markedly inhibited tumor cell proliferation *in vitro* and tumor growth *in vivo*. EMT

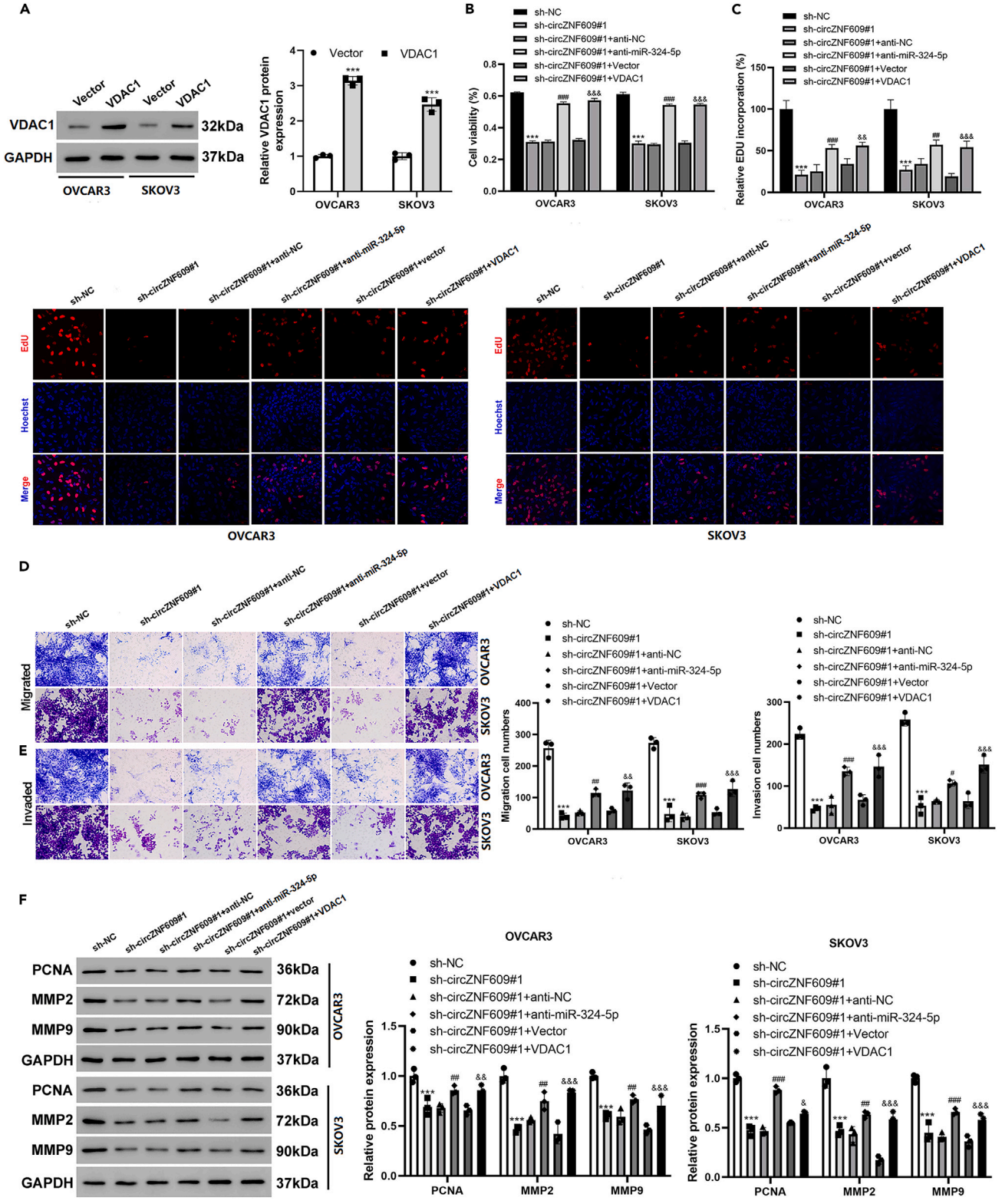
A
Vector
VDAC1
Vector
VDAC1
VDAC1
GAPDH
32kDa
37kDa
OVCAR3
SKOV3
Relative VDAC1 protein expression
Vector
VDAC1
OVCAR3
SKOV3
B
sh-NC
sh-circZNF609#1
sh-circZNF609#1+anti-NC
sh-circZNF609#1+anti-miR-324-5p
sh-circZNF609#1+Vector
sh-circZNF609#1+VDAC1
Cell viability (%)
OVCAR3
SKOV3
C
Relative EDU incorporation (%)
OVCAR3
SKOV3
EdU
Hoechst
Merge
OVCAR3
SKOV3
D
Migrated
OVCAR3
SKOV3
Migration cell numbers
E
Invaded
Invasion cell numbers
F
PCNA
MMP2
MMP9
GAPDH
36kDa
72kDa
90kDa
37kDa
OVCAR3
SKOV3
Relative protein expression

Figure 6. CircZNF609 promotes the malignant evolution of OC cells via miR-324-5p/VDAC1 axis

(A) The transfection efficiency of VDAC1 overexpression plasmid was measured by western blotting. CCK-8 assay (B), EdU assay (C), and Transwell assay (D and E) were used to assess cell proliferation, migration and invasion in OVCAR3 and SKOV3 cells following transfection with sh-NC, sh-circZNF609#1, sh-circZNF609#1 + anti-NC, sh-circZNF609#1 + anti-miR-324-5p, sh-circZNF609#1 + Vector, sh-circZNF609#1 +VDAC1.

(F) Western blotting was used to detect the protein levels of PCNA, MMP-2 and MMP-9 in OVCAR3 and SKOV3 cells following transfection with sh-NC, sh-circZNF609#1, sh-circZNF609#1 + anti-NC, sh-circZNF609#1 + anti-miR-324-5p, sh-circZNF609#1 + Vector, sh-circZNF609#1 +VDAC1. All data were presented as the mean ± SD of three independent experiments. ***$p < 0.001$ vs. Vector or sh-NC; $^{\#}p < 0.05$, $^{\#\#}p < 0.01$, $^{\#\#\#}p < 0.001$ vs. sh-circZNF609#1+anti-NC; $^{\&}p < 0.05$, $^{\&\&}p < 0.01$, $^{\&\&\&}p < 0.001$ vs. sh-circZNF609#1+Vector.

is a crucial process in cancer progression, where tumor cells transition from an epithelial to a mesenchymal state, enhancing their ability to migrate and invade.[39] This shift is marked by a decrease in E-cadherin and an increase in mesenchymal markers such as N-cadherin and Vimentin, driven by EMT transcription factors such as Twist1.[40,41] Our study reveals that silencing circZNF609 reverses this process, upregulating E-cadherin and downregulating N-cadherin, Vimentin, and Twist1, thereby reducing the metastatic potential of OC cells. Taken together, the *in vitro* and *in vivo* evidence demonstrated that circZNF609 promotes OC progression.

CircRNAs have emerged as pivotal players in biological processes, with their capacity to interact directly with proteins or function as miRNA sponges being pivotal mechanisms in their regulatory roles.[10,42] The circRNA-mediated ceRNA network has been pivotal in the therapeutic landscape of OC progression. For instance, Gong et al. demonstrated that circ9119 attenuates OC progression by sequestering miR-21-5p, thereby modulating the oncogenic pathway.[43] Similarly, Xu et al. identified circUBAP2 in OC, which targets miR-382-5p to promote OC tumorigenesis.[44] Moreover, Zhang et al. reported that CiRS-7 facilitates OC cell EMT by acting as a sponge for miR-641.[45] In our study, we identified miR-324-5p as a target of circZNF609, which was downregulated in OC tissues. Silencing circZNF609 to restore miR-324-5p expression was found to suppress OC cell glucose consumption, lactate production, proliferation, and tumor growth. Moreover, miR-324-5p has been confirmed to exert anti-oncogenic effects in OC by modulating cancer proliferation, migration, and invasion, echoing the previous

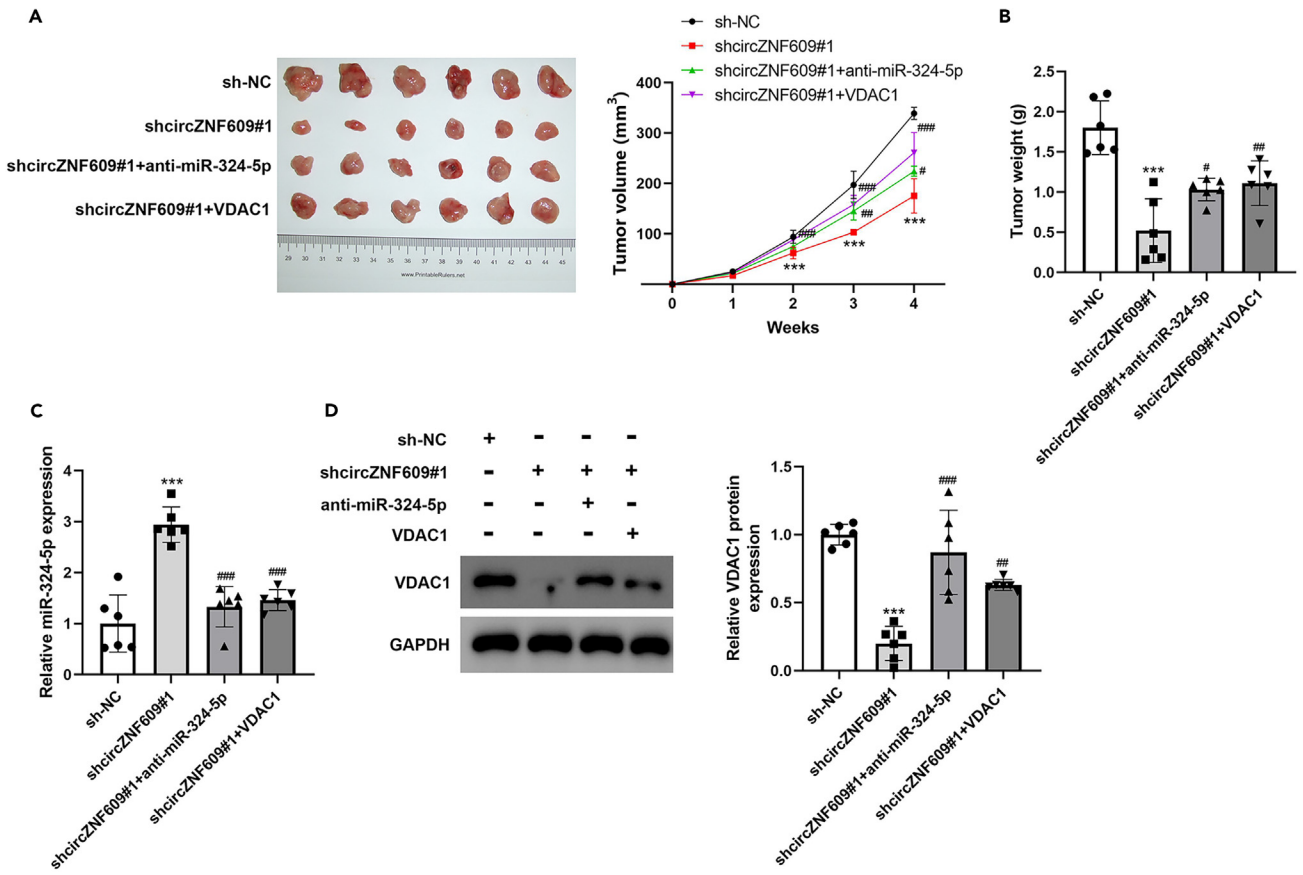

Figure 7. CircZNF609/miR-324-5p/VDAC1 axis regulated OC progression *in vivo*

SKOV3 cells transfected with sh-NC, sh-circZNF609#1, sh-circZNF609#1 + anti-miR-324-5p, and sh-circZNF609#1 + VDAC1 were subcutaneously injected into nude mice ($N = 6$ per group), and then the representative photographs of xenograft tumors were shown; the tumor volume (A) and weight (B) were assessed. The relative expression of miR-324-5p (C) and VDAC1 protein levels (D) were measured by qRT-PCR and western blotting, respectively. All data were presented as the mean ± SD of three independent experiments. ***$p < 0.001$ vs. sh-NC; $^{\#}p < 0.05$, $^{\#\#}p < 0.01$, $^{\#\#\#}p < 0.001$ vs. sh-circZNF609#1.

findings.[32] Our functional assays validated that miR-324-5p inhibition reversed the inhibitory effects of circZNF609 silencing on OC cell malignant phenotypes.

VDAC1 is a multifunctional protein located in the mitochondrial outer membrane, functioning as an ion channel.[46] Previous research has indicated that VDAC1 is overexpressed in a variety of cancers, including lung cancer,[47] cervical cancer,[48] and OC,[49] and is implicated in cellular metabolism. Our study aligned with these observations, confirming the elevated expression of VDAC1 in OC tissues. Pearson correlation analysis revealed a positive association between VDAC1 and circZNF609 expression, and a negative correlation with miR-324-5p expression in OC tissues, hinting at the presence of a ceRNA regulatory network involving circZNF609 in this context. Our research further substantiated the direct interaction between miR-324-5p and VDAC1. Rescue assays demonstrated that overexpression of VDAC1 counteracted the inhibitory effects on cell viability, migration, and invasion in OC cells induced by circZNF609 silencing, thus supporting our hypothesis that circZNF609 functions as a ceRNA to promote VDAC1-mediated proliferation, migration, and invasion by sequestering miR-324-5p in OC. Moreover, xenograft experiments indicated that the silencing of circZNF609 suppressed OC development *in vivo* by regulating CLU expression by acting as a sponge of miR-324-5p.

In conclusion, our study has demonstrated that circZNF609 can positively modulate the malignant behaviors of OC cells by sequestering miR-324-5p and upregulating VDAC1. These findings lay the groundwork for the discovery of molecular targets for the diagnosis and treatment of OC, offering a theoretical basis for future research in this area.

Limitations of the study

Despite the significant findings of our study, certain limitations must be acknowledged and addressed in future research. Firstly, while the expression of circZNF609 was assessed in a modest cohort of OC samples, a larger sample size is necessary to validate the correlation between circZNF609, miR-324-5p, and VDAC1 expression levels and various clinical parameters. This expansion would provide a more robust statistical basis for the clinical relevance of these molecular markers. Moreover, the potential presence of additional miRNA response elements within circZNF609 warrants further investigation. This exploration could uncover additional regulatory pathways that circZNF609 may influence, thereby enhancing our understanding of its role in OC. Furthermore, the effect of VDAC1 overexpression on the mitochondria requires further elucidation.

RESOURCE AVAILABILITY

Lead contact

Further information and requests for resources and reagents should be directed to and will be fulfilled by the Lead Contact, Yi Zhao (zhaoyicmu@sina.com).

Materials availability statement

Plasmids and/or cell lines generated in this study are available upon reasonable request. Please contact the lead contact.

Data and code availability

- All data reported in this article will be shared by the lead contact upon request.
- This article does not report original code.
- Any additional information required to reanalyze the data reported in this article is available from the lead contact upon request.

ACKNOWLEDGMENTS

Not applicable.

AUTHOR CONTRIBUTIONS

LR, XH, and YZ conceived the project and supervised all experiments. LR and YZ conducted all experiments and analyzed the data. XH provided support with experimental techniques. LR and YZ constructed the article. All authors read and approved the final article.

DECLARATION OF INTERESTS

The authors declare no competing interests.

STAR★METHODS

Detailed methods are provided in the online version of this paper and include the following:

- KEY RESOURCES TABLE
- EXPERIMENTAL MODEL AND STUDY PARTICIPANT DETAILS
  - Clinical specimens
  - Xenograft assay
- METHOD DETAILS
  - Cell culture
  - Transfection
  - QRT-PCR analysis
  - Western blot

- CCK-8 assay
- EdU assay
- Transwell assays
- Bioinformatics analysis
- Luciferase reporter assay
- RNA pull-down assay

- QUANTIFICATION AND STATISTICAL ANALYSIS
- ADDITIONAL RESOURCES

SUPPLEMENTAL INFORMATION

Supplemental information can be found online at https://doi.org/10.1016/j.isci.2024.110861.

Received: March 30, 2024
Revised: August 3, 2024
Accepted: August 29, 2024
Published: August 31, 2024

REFERENCES

1. Webb, P.M., and Jordan, S.J. (2024). Global epidemiology of epithelial ovarian cancer. Nat. Rev. Clin. Oncol. *21*, 389–400. https://doi.org/10.1038/s41571-024-00881-3.
2. Straubhar, A., Chi, D.S., and Long Roche, K. (2020). Update on the role of surgery in the management of advanced epithelial ovarian cancer. Clin. Adv. Hematol. Oncol. *18*, 723–731.
3. Christie, E.L., and Bowtell, D.D.L. (2017). Acquired chemotherapy resistance in ovarian cancer. Ann. Oncol. *28*, viii13–viii15. https://doi.org/10.1093/annonc/mdx446.
4. Guan, L.Y., and Lu, Y. (2018). New developments in molecular targeted therapy of ovarian cancer. Discov. Med. *26*, 219–229.
5. Patop, I.L., Wüst, S., and Kadener, S. (2019). Past, present, and future of circRNAs. EMBO J. *38*, e100836. https://doi.org/10.15252/embj.2018100836.
6. Sanger, H.L., Klotz, G., Riesner, D., Gross, H.J., and Kleinschmidt, A.K. (1976). Viroids are single-stranded covalently closed circular RNA molecules existing as highly base-paired rod-like structures. Proc. Natl. Acad. Sci. USA *73*, 3852–3856. https://doi.org/10.1073/pnas.73.11.3852.
7. Kristensen, L.S., Andersen, M.S., Stagsted, L.V.W., Ebbesen, K.K., Hansen, T.B., and Kjems, J. (2019). The biogenesis, biology and characterization of circular RNAs. Nat. Rev. Genet. *20*, 675–691. https://doi.org/10.1038/s41576-019-0158-7.
8. Han, B., Chao, J., and Yao, H. (2018). Circular RNA and its mechanisms in disease: From the bench to the clinic. Pharmacol. Ther. *187*, 31–44. https://doi.org/10.1016/j.pharmthera.2018.01.010.
9. Zang, J., Lu, D., and Xu, A. (2020). The interaction of circRNAs and RNA binding proteins: An important part of circRNA maintenance and function. J. Neurosci. Res. *98*, 87–97. https://doi.org/10.1002/jnr.24356.
10. Panda, A.C. (2018). Circular RNAs Act as miRNA Sponges. Adv. Exp. Med. Biol. *1087*, 67–79. https://doi.org/10.1007/978-981-13-1426-1_6.
11. Zhang, H.D., Jiang, L.H., Sun, D.W., Hou, J.C., and Ji, Z.L. (2018). CircRNA: a novel type of biomarker for cancer. Breast Cancer *25*, 1–7. https://doi.org/10.1007/s12282-017-0793-9.
12. Goodall, G.J., and Wickramasinghe, V.O. (2021). RNA in cancer. Nat. Rev. Cancer *21*, 22–36. https://doi.org/10.1038/s41568-020-00306-0.
13. Yang, X., Mei, J., Wang, H., Gu, D., Ding, J., and Liu, C. (2020). The emerging roles of circular RNAs in ovarian cancer. Cancer Cell Int. *20*, 265. https://doi.org/10.1186/s12935-020-01367-9.
14. Sheng, R., Li, X., Wang, Z., and Wang, X. (2020). Circular RNAs and their emerging roles as diagnostic and prognostic biomarkers in ovarian cancer. Cancer Lett. *473*, 139–147. https://doi.org/10.1016/j.canlet.2019.12.043.
15. He, Y., Huang, H., Jin, L., Zhang, F., Zeng, M., Wei, L., Tang, S., Chen, D., and Wang, W. (2020). CircZNF609 enhances hepatocellular carcinoma cell proliferation, metastasis, and stemness by activating the Hedgehog pathway through the regulation of miR-15a-5p/15b-5p and GLI2 expressions. Cell Death Dis. *11*, 358. https://doi.org/10.1038/s41419-020-2441-0.
16. Gu, Q., Hou, W., Shi, L., Liu, H., Zhu, Z., and Ye, W. (2021). Circular RNA ZNF609 functions as a competing endogenous RNA in regulating E2F transcription factor 6 through competitively binding to microRNA-197-3p to promote the progression of cervical cancer progression. Bioengineered *12*, 927–936. https://doi.org/10.1080/21655979.2021.1896116.
17. Wang, S., Xue, X., Wang, R., Li, X., Li, Q., Wang, Y., Xie, P., Kang, Y., Meng, R., and Feng, X. (2018). CircZNF609 promotes breast cancer cell growth, migration, and invasion by elevating p70S6K1 via sponging miR-145-5p. Cancer Manag. Res. *10*, 3881–3890. https://doi.org/10.2147/CMAR.S174778.
18. Jin, C., Zhao, W., Zhang, Z., and Liu, W. (2019). Silencing circular RNA circZNF609 restrains growth, migration and invasion by up-regulating microRNA-186-5p in prostate cancer. Artif. Cells, Nanomed. Biotechnol. *47*, 3350–3358. https://doi.org/10.1080/21691401.2019.1648281.
19. Du, S., Zhang, P., Ren, W., Yang, F., and Du, C. (2020). Circ-ZNF609 Accelerates the Radioresistance of Prostate Cancer Cells by Promoting the Glycolytic Metabolism Through miR-501-3p/HK2 Axis. Cancer Manag. Res. *12*, 7487–7499. https://doi.org/10.2147/CMAR.S257441.
20. Wu, W., Wei, N., Shao, G., Jiang, C., Zhang, S., and Wang, L. (2019). circZNF609 promotes the proliferation and migration of gastric cancer by sponging miR-483-3p and regulating CDK6. OncoTargets Ther. *12*, 8197–8205. https://doi.org/10.2147/OTT.S193031.
21. Liu, Z., Pan, H.M., Xin, L., Zhang, Y., Zhang, W.M., Cao, P., and Xu, H.W. (2019). Circ-ZNF609 promotes carcinogenesis of gastric cancer cells by inhibiting miRNA-145-5p expression. Eur. Rev. Med. Pharmacol. Sci. *23*, 9411–9417. https://doi.org/10.26355/eurrev_201911_19433.
22. Liu, S., Yang, N., Jiang, X., Wang, J., Dong, J., and Gao, Y. (2021). FUS-induced circular RNA ZNF609 promotes tumorigenesis and progression via sponging miR-142-3p in lung cancer. J. Cell. Physiol. *236*, 79–92. https://doi.org/10.1002/jcp.29481.
23. Wang, F., Li, X., Jia, X., and Geng, L. (2021). CircRNA ZNF609 Knockdown Represses the Development of Non-Small Cell Lung Cancer via miR-623/FOXM1 Axis. Cancer Manag. Res. *13*, 1029–1039. https://doi.org/10.2147/CMAR.S282162.
24. Tong, H., Zhao, K., Wang, J., Xu, H., and Xiao, J. (2020). CircZNF609/miR-134-5p/BTG-2 axis regulates proliferation and migration of glioma cell. J. Pharm. Pharmacol. *72*, 68–75. https://doi.org/10.1111/jphp.13188.
25. Du, S., Li, H., Lu, F., Zhang, S., and Tang, J. (2021). Circular RNA ZNF609 promotes the malignant progression of glioma by regulating miR-1224-3p/PLK1 signaling. J. Cancer *12*, 3354–3366. https://doi.org/10.7150/jca.54934.
26. Cui, M., Liu, Y., Cheng, L., Li, T., Deng, Y., and Liu, D. (2022). Research progress on anti-ovarian cancer mechanism of miRNA regulating tumor microenvironment. Front. Immunol. *13*, 1050917. https://doi.org/10.3389/fimmu.2022.1050917.
27. Ali Syeda, Z., Langden, S.S.S., Munkhzul, C., Lee, M., and Song, S.J. (2020). Regulatory Mechanism of MicroRNA Expression in Cancer. Int. J. Mol. Sci. *21*, 1723. https://doi.org/10.3390/ijms21051723.
28. Li, D., Li, L., Chen, X., Yang, W., and Cao, Y. (2021). Circular RNA SERPINE2 promotes development of glioblastoma by regulating the miR-361-3p/miR-324-5p/BCL2 signaling pathway. Mol. Ther. Oncolytics *22*, 483–494. https://doi.org/10.1016/j.omto.2021.07.010.
29. Wang, P., Wang, T., Dong, L., Xu, Z., Guo, S., and Chang, C. (2022). Circular RNA circ_0079593 facilitates glioma development via modulating miR-324-5p/XBP1 axis. Metab. Brain Dis. *37*, 2389–2403. https://doi.org/10.1007/s11011-022-01040-2.

30. Lin, H., Zhou, A.J., Zhang, J.Y., Liu, S.F., and Gu, J.X. (2018). MiR-324-5p reduces viability and induces apoptosis in gastric cancer cells through modulating TSPAN8. J. Pharm. Pharmacol. *70*, 1513–1520. https://doi.org/10.1111/jphp.12995.
31. Xie, Y., Liu, Z., and Zhu, H. (2021). Knockdown of hsa_circ_0091994 constrains gastric cancer progression by suppressing the miR-324-5p/HMGA1 axis. Aging (Albany NY) *13*, 20598–20608. https://doi.org/10.18632/aging.203450.
32. Zheng, X., Zhou, Y., Chen, W., Chen, L., Lu, J., He, F., Li, X., and Zhao, L. (2018). Ginsenoside 20(S)-Rg3 Prevents PKM2-Targeting miR-324-5p from H19 Sponging to Antagonize the Warburg Effect in Ovarian Cancer Cells. Cell. Physiol. Biochem. *51*, 1340–1353. https://doi.org/10.1159/000495552.
33. Suardi, R.B., Ysrafil, Y., Sesotyosari, S.L., Martien, R., Wardana, T., Astuti, I., and Haryana, S.M. (2020). The Effects of Combination of Mimic miR-155-5p and Antagonist miR-324-5p Encapsulated Chitosan in Ovarian Cancer SKOV3. Asian Pac. J. Cancer Prev. *21*, 2603–2608. https://doi.org/10.31557/apjcp.2020.21.9.2603.
34. Shoshan-Barmatz, V., Shteinfer-Kuzmine, A., and Verma, A. (2020). VDAC1 at the Intersection of Cell Metabolism, Apoptosis, and Diseases. Biomolecules *10*, 1485. https://doi.org/10.3390/biom10111485.
35. Li, Y., Kang, J., Fu, J., Luo, H., Liu, Y., Li, Y., and Sun, L. (2021). PGC1α Promotes Cisplatin Resistance in Ovarian Cancer by Regulating the HSP70/HK2/VDAC1 Signaling Pathway. Int. J. Mol. Sci. *22*, 2537. https://doi.org/10.3390/ijms22052537.
36. Momenimovahed, Z., Tiznobaik, A., Taheri, S., and Salehiniya, H. (2019). Ovarian cancer in the world: epidemiology and risk factors. Int. J. Womens Health *11*, 287–299. https://doi.org/10.2147/IJWH.S197604.
37. Kuroki, L., and Guntupalli, S.R. (2020). Treatment of epithelial ovarian cancer. BMJ *371*, m3773. https://doi.org/10.1136/bmj.m3773.
38. Shabaninejad, Z., Vafadar, A., Movahedpour, A., Ghasemi, Y., Namdar, A., Fathizadeh, H., Pourhanifeh, M.H., Savardashtaki, A., and Mirzaei, H. (2019). Circular RNAs in cancer: new insights into functions and implications in ovarian cancer. J. Ovarian Res. *12*, 84. https://doi.org/10.1186/s13048-019-0558-5.
39. Bakir, B., Chiarella, A.M., Pitarresi, J.R., and Rustgi, A.K. (2020). EMT, MET, Plasticity, and Tumor Metastasis. Trends Cell Biol. *30*, 764–776. https://doi.org/10.1016/j.tcb.2020.07.003.
40. Li, Y., Zhang, T., Qin, S., Wang, R., Li, Y., Zhou, Z., Chen, Y., Wu, Q., and Su, F. (2019). Effects of UPF1 expression on EMT process by targeting E-cadherin, N-cadherin, Vimentin and Twist in a hepatocellular carcinoma cell line. Mol. Med. Rep. *19*, 2137–2143. https://doi.org/10.3892/mmr.2019.9838.
41. Luo, D., Zeng, X., Zhang, S., Li, D., Cheng, Z., Wang, Y., Long, J., Hu, Z., Long, S., Zhou, J., et al. (2023). Pirfenidone suppressed triple-negative breast cancer metastasis by inhibiting the activity of the TGF-β/SMAD pathway. J. Cell Mol. Med. *27*, 456–469. https://doi.org/10.1111/jcmm.17673.
42. Du, W.W., Zhang, C., Yang, W., Yong, T., Awan, F.M., and Yang, B.B. (2017). Identifying and Characterizing circRNA-Protein Interaction. Theranostics *7*, 4183–4191. https://doi.org/10.7150/thno.21299.
43. Gong, J., Xu, X., Zhang, X., and Zhou, Y. (2020). Circular RNA-9119 suppresses in ovarian cancer cell viability via targeting the microRNA-21-5p-PTEN-Akt pathway. Aging (Albany NY) *12*, 14314–14328. https://doi.org/10.18632/aging.103470.
44. Xu, Q., Deng, B., Li, M., Chen, Y., and Zhuan, L. (2020). circRNA-UBAP2 promotes the proliferation and inhibits apoptosis of ovarian cancer though miR-382-5p/PRPF8 axis. J. Ovarian Res. *13*, 81. https://doi.org/10.1186/s13048-020-00685-w.
45. Zhang, F., Xu, Y., Ye, W., Jiang, J., and Wu, C. (2020). Circular RNA S-7 promotes ovarian cancer EMT via sponging miR-641 to up-regulate ZEB1 and MDM2. Biosci. Rep. *40*, BSR20200825. https://doi.org/10.1042/BSR20200825.
46. Shoshan-Barmatz, V., De Pinto, V., Zweckstetter, M., Raviv, Z., Keinan, N., and Arbel, N. (2010). VDAC, a multi-functional mitochondrial protein regulating cell life and death. Mol. Aspect. Med. *31*, 227–285. https://doi.org/10.1016/j.mam.2010.03.002.
47. Zhang, G., Jiang, G., Wang, C., Zhong, K., Zhang, J., Xue, Q., Li, X., Jin, H., and Li, B. (2016). Decreased expression of microRNA-320a promotes proliferation and invasion of non-small cell lung cancer cells by increasing VDAC1 expression. Oncotarget *7*, 49470–49480. https://doi.org/10.18632/oncotarget.9943.
48. Zhang, C., Ding, W., Liu, Y., Hu, Z., Zhu, D., Wang, X., Yu, L., Wang, L., Shen, H., Zhang, W., et al. (2016). Proteomics-based identification of VDAC1 as a tumor promoter in cervical carcinoma. Oncotarget *7*, 52317–52328. https://doi.org/10.18632/oncotarget.10562.
49. Li, Y., Kang, J., Fu, J., Luo, H., Liu, Y., Li, Y., and Sun, L. (2021). PGC1alpha Promotes Cisplatin Resistance in Ovarian Cancer by Regulating the HSP70/HK2/VDAC1 Signaling Pathway. Int. J. Mol. Sci. *22*, 2537. https://doi.org/10.3390/ijms22052537.
50. Dudekula, D.B., Panda, A.C., Grammatikakis, I., De, S., Abdelmohsen, K., and Gorospe, M. (2016). CircInteractome: A web tool for exploring circular RNAs and their interacting proteins and microRNAs. RNA Biol. *13*, 34–42. https://doi.org/10.1080/15476286.2015.1128065.
51. Li, J.H., Liu, S., Zhou, H., Qu, L.H., and Yang, J.H. (2014). starBase v2.0: decoding miRNA-ceRNA, miRNA-ncRNA and protein-RNA interaction networks from large-scale CLIP-Seq data. Nucleic Acids Res. *42*, D92–D97. https://doi.org/10.1093/nar/gkt1248.

STAR★METHODS

KEY RESOURCES TABLE

REAGENT or RESOURCE	SOURCE	IDENTIFIER
Antibodies		
VDAC1	Cell Signaling Technology	Cat# 4661; RRID: AB_10557420
PCNA	Cell Signaling Technology	Cat# 13110; RRID: AB_2636979
MMP-2	Cell Signaling Technology	Cat# 40994; RRID: AB_2799191
MMP-9	Cell Signaling Technology	Cat# 13667; RRID: AB_2798289
E-cadherin	Cell Signaling Technology	Cat# 3195; RRID: AB_2291471
N-cadherin	Cell Signaling Technology	Cat# 13116; RRID: AB_2687616
Vimentin	Cell Signaling Technology	Cat# 5741; RRID: AB_10695459
Twist1	Cell Signaling Technology	Cat# 90445; RRID: AB_3064916
GAPDH	Cell Signaling Technology	Cat# 5174; RRID: AB_10622025
IgG secondary antibody	Cell Signaling Technology	Cat# 7074; RRID: AB_2099233
Biological samples		
Fouty pairs of OC and adjacent normal tissues	The First Hospital of China Medical University	N/A
Chemicals, peptides, and recombinant proteins		
Lipofectamine 3000	Invitrogen	Cat# L3000001
Trizol reagent	Invitrogen	Cat# 15596018CN
RIPA	Beyotime Biotechnology	Cat# P0013B
chemiluminescence reagent	Beyotime Biotechnology	Cat# P0018S
Critical commercial assays		
CCK-8	Beyotime Biotechnology	Cat# C0038
BeyoClick™ EdU Cell Proliferation Kit	Beyotime Biotechnology	Cat# C0071S
High-Capacity cDNA Reverse Transcription Kit	Applied Biosystems	Cat# 4368814
PrimeScript™ RT Master Mix	Takara	Cat# RR036A
Enhanced BCA Protein Assay Kit	Beyotime Biotechnology	Cat# P0009
Pierce Renilla-Firefly Luciferase Dual Assay Kit	Thermo Scientific	Cat# 16186
Pierce Magnetic RNA-Protein Pull-Down Kit	Thermo Scientific	Cat# 20164
Deposited data		
CircInteractome database	CircInteractome	https://circinteractome.nia.nih.gov/
ENCORI Pan-Cancer Analysis Platform	ENCORI	https://starbase.sysu.edu.cn/
Experimental models: Cell lines		
HOSEpic	ScienCell	Cat# 7310
CAOV3	Cell Bank of the Chinese Academy of Sciences	Cat# SCSP-570
A2780	Cell Bank of the Chinese Academy of Sciences	Cat# CC-Y1557
OVCAR3	Cell Bank of the Chinese Academy of Sciences	Cat# SCSP-558
SKOV3	Cell Bank of the Chinese Academy of Sciences	Cat# SCSP-5214
Experimental models: Organisms/strains		
BALB/c female nude mice	Experimental Animal Center of The First Hospital of China Medical University	N/A
Oligonucleotides		
sh-circZNF609#1: 5′-AGUCUGAAAAGCAAUGAUGUU-3′	This paper	N/A
sh-circZNF609#2: 5′-GUCUGAAAAGCAAUGAUGUUG-3′	This paper	N/A

(*Continued on next page*)

Continued

REAGENT or RESOURCE	SOURCE	IDENTIFIER
sh-circZNF609#3: 5′-CAAGUCUGAAAAGCAAUGAUG-3′	This paper	N/A
sh-NC: 5′-AAGACAUUGUGUGUCCGCCTT-3′	This paper	N/A
miR-324-5p mimics: sense, 5′-CGCAUCCCCUAGGGC AUUGGUGU-3′, antisense, 5′-ACCAAUGCCCUAG GGGAUGCGUU-3′	This paper	N/A
miR-NC: sense, 5′-UUCUCCGAACGUGUCACGUTT-3′, antisense, 5′-ACGUGACACGUUCGGAGAATT-3′	This paper	N/A
anti-miR-324-5p: 5′-ACACCAAUGCCCUAGGGGAUGCG-3′	This paper	N/A
anti-NC: 5′-CAGUACUUUUGUGUAGUACAA-3′	This paper	N/A
circZNF609 forward: 5'-CAGCGCTCAATCCTTTGGGA-3', reverse: 5'-GACCTGCCACATTGGTCAGTA-3'	This paper	N/A
miR-324-5p forward 5′-ACACTCCAGCTGGGCGCA TCCCCTAGGGCAT-3′, reverse 5′-TGG TGTCGTGGAGTCG-3′	This paper	N/A
VDAC1 forward 5'-ACGTATGCCGATCTTGGCAAA-3', reverse 5'-TCAGGCCGTACTCAGTCCATC-3'	This paper	N/A
GAPDH forward 5'-GGAGCGAGATCCCTCCAAAAT-3', reverse 5'-GGCTGTTGTCATACTTCTCATGG-3'	This paper	N/A
U6 forward 5'-CTCGCTTCGGCAGCACATATACT-3', reverse 5'-ACGCTTCACGAATTTGCGTGTC-3'	This paper	N/A
Software and algorithms		
SPSS 19.0	IBM	http://www.ibm.com/cn/

EXPERIMENTAL MODEL AND STUDY PARTICIPANT DETAILS

Clinical specimens

Our research was granted ethical approval by the Ethical Committee of The First Hospital of China Medical University, with the approval number [2021]491. We procured 40 pairs of tumor and adjacent normal tissues from patients with OC who underwent surgical intervention during their hospital stay, following the acquisition of informed consent. The inclusion criteria were as follows: OC was confirmed by pathological examination, all cases of OC were non-metastatic and none of the patients had received chemoradiotherapy or radiotherapy prior to surgery. The exclusion criteria were as follows: Patients with metastatic tumors and/or those who had received prior chemoradiotherapy or radiotherapy. Patient information is listed in Table S1.

Xenograft assay

The Animal Care and Use Committee of The First Hospital of China Medical University approved this study. Equal numbers of 3×10^6 SKOV3 viable cells transfected with sh-NC, sh-circZNF609#1, shcircZNF609#1 plus anti-miR-324-5p, or shcircZNF609 plus VDAC1 were suspended in 100 μL and injected subcutaneously into the posterior right flanks of 6-week-old female BALB/c nude mice, with six mice per group. Tumor volume was measured every 7 days. Four weeks later, the mice were sacrificed and tumors were removed for further analysis.

METHOD DETAILS

Cell culture

The normal human ovarian epithelial cell line HOSEpiC and four ovarian cancer cell lines (CAOV3, A2780, OVCAR3, and SKOV3) were procured from ScienCell Research Laboratories (Carlsbad, CA, USA) and the Cell Bank of the Chinese Academy of Sciences (Shanghai, China), respectively. Cultured in Dulbecco's Modified Eagle's Medium (DMEM; Invitrogen, Carlsbad, CA, USA) supplemented with 10% fetal bovine serum (FBS; Gibco, Carlsbad, CA, USA), 1% penicillin/streptomycin (Gibco), and 0.01 mg/mL bovine insulin, the cells were maintained at 37°C in an atmosphere of 95% air and 5% CO_2.

Transfection

The shRNAs targeting circZNF609 (sh-circZNF609#1, 5′-AGUCUGAAAAGCAAUGAUGUU-3′; sh-circZNF609#2, 5′-GUCUGAAAAGCAAUGAUGUUG-3′; sh-circZNF609#3, 5′-CAAGUCUGAAAAGCAAUGAUG-3′), the negative control shRNA (sh-NC, 5′-AAGACAUUGUGUGUCCGCCTT-3′), the miR-324-5p mimics (sense, 5′-CGCAUCCCCUAGGGCAUUGGUGU-3′; antisense, 5′-ACCAAUGCCCUAGGGGAUGCGUU-3′), the negative control miRNA (miR-NC, sense, 5′-UUCUCCGAACGUGUCACGUTT-3′; antisense, 5′-ACGUGACACGUUCGGAGAATT-3′), the anti-miR-324-5p inhibitor (5′-ACACCAAUGCCCUAGGGGAUGCG-3′), and the negative control inhibitor (anti-NC, 5′-CAGUACUUUUGUGUAGUACAA-3′) were synthesized by GenePharma Co., Ltd (Shanghai, China). The full-length sequences of VDAC1 were cloned into the pcDNA3.1 vector (Invitrogen) to construct the VDAC1 overexpression vector. Upon reaching approximately 70% confluence, the cells were transfected with the aforementioned shRNAs, miRNA mimics, inhibitors, and the overexpression vector using Lipofectamine 3000 (Invitrogen) in accordance with the manufacturer's protocol. After 48 h of transfection, the transfection efficiency was assessed using real-time PCR and western blotting.

QRT-PCR analysis

Total RNA was isolated using Trizol reagent (Invitrogen), and subsequently, cDNA was synthesized using the High-Capacity cDNA Reverse Transcription Kit (Applied Biosystems, Carlsbad, CA, USA). The PCR reaction was performed using PrimeScript RT Master Mix (Takara, Beijing, China) on an Applied Biosystems Real-Time PCR System, following the manufacturer's guidelines. GAPDH served as the internal control for VDAC1 and circZNF609, while U6 was chosen as the internal control for miR-324-5p. The relative expression levels were quantified using the $2^{-\Delta\Delta CT}$ method. The reverse transcription primers for circZNF609, miR-324-5p, VDAC1, GAPDH, and U6 were listed in Table S2.

Western blot

Protein extraction from tissues and cell lines was performed using RIPA buffer supplemented with a protease inhibitor cocktail (Beyotime Biotechnology, Shanghai, China). Protein quantification was conducted using the Enhanced BCA Protein Assay Kit (Beyotime Biotechnology). Subsequently, 10 μg of protein was resolved on 10% polyacrylamide gels and transferred onto polyvinylidene fluoride (PVDF) membranes. Following a 1-h block in a 5% non-fat milk solution in Tris-buffered saline with Tween 20 at room temperature, the membranes were incubated with primary antibodies against VDAC1 (#4661), PCNA (#13110), MMP-2 (#40994), MMP-9 (#13667), E-cadherin (#3195), N-cadherin (#13116), Vimentin (#5741), Twist1 (#90445), and GAPDH (#5174) at a 1/1000 dilution, and subsequently with HRP-conjugated goat anti-rabbit IgG (#7074) at a 1/2000 dilution (Cell Signaling Technology, Boston, MA, USA). Protein bands were visualized using chemiluminescence reagent (Beyotime Biotechnology).

CCK-8 assay

Following transfection, 2000 cells of the appropriate OC cell line were seeded into each well of a 96-well plate, with six wells allocated per experimental group. The cells were then subjected to the CCK-8 assay after 24 h. The assay was conducted by incubating the cells with 10 μL of CCK-8 reagent (Beyotime Biotechnology) for 2 h, and the absorbance was measured at 450 nm.

EdU assay

The EdU incorporation assay was conducted using the BeyoClick EdU Cell Proliferation Kit (Beyotime Biotechnology). After transfection, OC cells were seeded into 96-well plates at a density of 1 × 10^5 cells per well. Cells were incubated in 10 μM EdU labeling media for 2 h to allow for the incorporation of EdU into newly synthesized DNA. Following this, the cells were fixed with 4% paraformaldehyde in PBS and permeabilized with 0.5% Triton X-100. Subsequently, the cells were stained with Apollo dye solution for 30 min to visualize the EdU-labeled DNA, and then counterstained with Hoechst 33342 for an additional 30 min at room temperature to label all nuclei. The stained cells were imaged using a microscope (Olympus, Tokyo, Japan), and the proportion of EdU-positive cells was quantified using ImageJ software.

Transwell assays

The migratory and invasive capabilities of OC cells were assessed using 8 μm pore size Transwell chambers (Corning Inc., Corning, NY, USA) for migration assays and Matrigel-coated Transwell chambers for invasion assays. For both assays, 200 μL of a cell suspension containing 1 × 10^5 cells was introduced into the upper chamber, while the lower chamber was filled with 600 μL of DMEM supplemented with 10% FBS. Following a 24-h incubation period, the cells in the upper chamber were fixed with 4% paraformaldehyde for 20 min and subsequently stained with 1% crystal violet. Non-migrated and non-invaded cells were removed, and the remaining cells were photographed and quantified under a microscope at 200× magnification across five randomly selected fields.

Bioinformatics analysis

To elucidate the potential interactions between circZNF609 and miR-324-5p, as well as the binding sites of miR-324-5p on the 3′UTR of VDAC1, we employed the CircInteractome database (https://circinteractome.nia.nih.gov/)[50] and ENCORI Pan-Cancer Analysis Platform (https://starbase.sysu.edu.cn/)[51] online platforms. CircInteractome is a specialized tool for predicting interactions between circRNAs and miRNAs, while ENCORI is a repository for identifying miRNA binding sites on mRNA 3′UTRs. Utilizing these computational resources, we aimed to construct a putative ceRNA network that could reveal the regulatory role of circZNF609 on VDAC1 expression through miR-324-5p.

Luciferase reporter assay

To investigate the interaction between miR-324-5p and its putative targets, OVCAR3 and SKOV3 cells were seeded into 24-well plates and subsequently transfected with wild-type or mutant luciferase reporter vectors containing the circZNF609 or VDAC1 3′-UTR sequences, which were cloned into the pGL6-miR vector (Beyotime Biotechnology). Upon reaching 70–80% confluency, 400 ng of the respective wild-type or mutant luciferase reporter vector was introduced into the cells, which were then co-transfected with 50 nM of miR-324-5p mimics or miR-NC for 24 h. The luciferase activity was quantified using the Pierce Renilla-Firefly Luciferase Dual Assay Kit (Thermo Scientific, Shanghai, China).

RNA pull-down assay

RNA pull-down analysis was performed using Pierce Magnetic RNA-Protein Pull-Down Kit (Thermo Scientific). After 24h transfection with biotinylated miR-324-5p or negative control (Bio-NC), the cell lysates of OVCAR3 and SKOV3 cells were collected and interacted with streptavidin-conjugated magnetic beads. The RNA complexes bound to the beads were eluted and extracted for qRT-PCR analysis to evaluate the relative enrichment of circZNF609.

QUANTIFICATION AND STATISTICAL ANALYSIS

The data presented were the aggregate results of a minimum of three independent experiments, expressed as mean ± standard deviation (SD). Statistical analyses were conducted using SPSS 19.0 (IBM, Chicago, IL, USA). The Student's *t*-test was employed to assess the significance of differences between two groups, whereas one-way analysis of variance (ANOVA) was followed by Tukey's post hoc test to evaluate variations across multiple groups. A P-value of less than 0.05 was deemed statistically significant. The 5-year survival curve was generated using the Kaplan-Meier method. Pearson correlation analysis was utilized to determine the expression correlation.

ADDITIONAL RESOURCES

Clinical samples of this study were obtained from diagnosed OC patients who underwent surgical resection, and the study protocol was approved by the ethics committee of The First Hospital of China Medical University (approval No. [2021]491). The animal experiment was supported by the Animal Care and Use Committee of The First Hospital of China Medical University.